Article

Current Biology

Regulation of the Elongation Phase of Protein Synthesis Enhances Translation Accuracy and Modulates Lifespan

Graphical Abstract

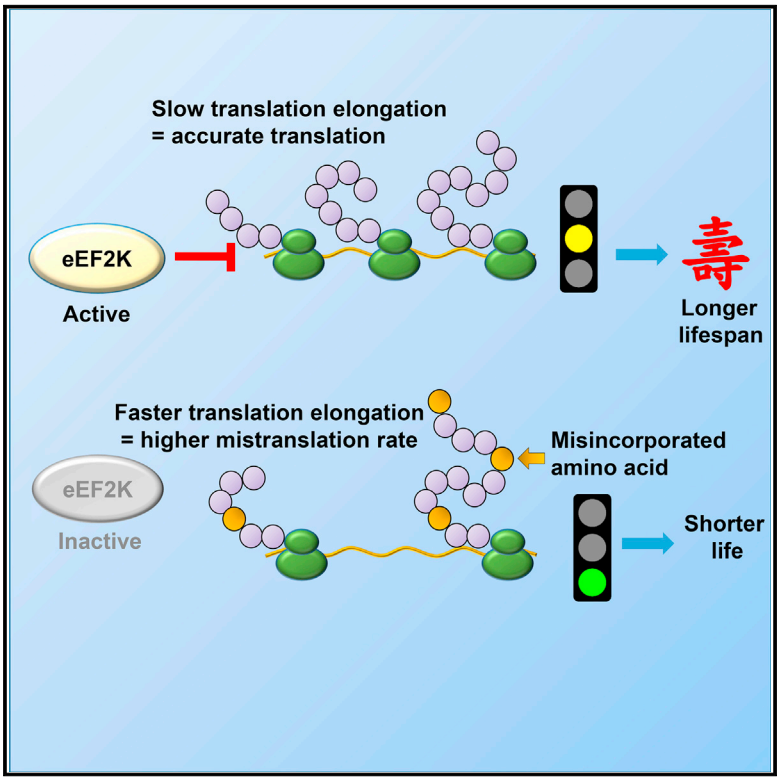

Authors

Jianling Xie, Viviane de Souza Alves, Tobias von der Haar, ..., Mark J. Coldwell, Xuemin Wang, Christopher G. Proud

Correspondence

christopher.proud@sahmri.com

In Brief

Xie et al. report that eukaryotic elongation factor 2 kinase (eEF2K), which impairs the rate of elongation, decreases misreading or termination readthrough errors and promotes the correct recognition of start codons in mRNAs. Depletion of the eEF2K ortholog or other factors implicated in translation fidelity in *C. elegans* decreases lifespan.

Highlights

- eEF2 kinase enhances the accuracy of protein synthesis under a range of conditions
- mTORC1 inhibition improves translation accuracy by activating eEF2K
- eEF2K assists correct start codon selection during translation initiation
- Impairing translation fidelity reduces lifespan in *C. elegans*

Xie et al., 2019, Current Biology *29*, 737–749
March 4, 2019
https://doi.org/10.1016/j.cub.2019.01.029

CellPress

Current Biology
Article

Regulation of the Elongation Phase of Protein Synthesis Enhances Translation Accuracy and Modulates Lifespan

Jianling Xie,[1,2] Viviane de Souza Alves,[3] Tobias von der Haar,[4] Louise O'Keefe,[5,6] Roman V. Lenchine,[1,5] Kirk B. Jensen,[1,5] Rui Liu,[1,2,7] Mark J. Coldwell,[2] Xuemin Wang,[1,2] and Christopher G. Proud[1,2,5,6,8,*]
[1]Nutrition & Metabolism, South Australian Health & Medical Research Institute, Adelaide, SA, Australia
[2]Centre for Biological Sciences, University of Southampton, Southampton, UK
[3]Departamento de Microbiologia, Universidade Federal de Minas Gerais, Belo Horizonte, MG, Brazil
[4]School of Biosciences, University of Kent, Canterbury, UK
[5]School of Biological Sciences, University of Adelaide, Adelaide, SA, Australia
[6]Hopwood Centre for Neurobiology, South Australian Health & Medical Research Institute, Adelaide, SA, Australia
[7]Present address: Molecular Genetics Unit, St. Vincent's Institute of Medical Research, Fitzroy, VIC, Australia
[8]Lead Contact
*Correspondence: christopher.proud@sahmri.com
https://doi.org/10.1016/j.cub.2019.01.029

SUMMARY

Maintaining accuracy during protein synthesis is crucial to avoid producing misfolded and/or non-functional proteins. The target of rapamycin complex 1 (TORC1) pathway and the activity of the protein synthesis machinery are known to negatively regulate lifespan in many organisms, although the precise mechanisms involved remain unclear. Mammalian TORC1 signaling accelerates the elongation stage of protein synthesis by inactivating eukaryotic elongation factor 2 kinase (eEF2K), which, when active, phosphorylates and inhibits eEF2, which mediates the movement of ribosomes along mRNAs, thereby slowing down the rate of elongation. We show that eEF2K enhances the accuracy of protein synthesis under a range of conditions and in several cell types. For example, our data reveal it links mammalian (m)TORC1 signaling to the accuracy of translation. Activation of eEF2K decreases misreading or termination readthrough errors during elongation, whereas knocking down or knocking out eEF2K increases their frequency. eEF2K also promotes the correct recognition of start codons in mRNAs. Reduced translational fidelity is known to correlate with shorter lifespan. Consistent with this, deletion of the eEF2K ortholog or other factors implicated in translation fidelity in *Caenorhabditis elegans* decreases lifespan, and eEF2K is required for lifespan extension induced by nutrient restriction. Our data uncover a novel mechanism linking nutrient supply, mTORC1 signaling, and the elongation stage of protein synthesis, which enhances the accuracy of protein synthesis. Our data also indicate that modulating translation elongation and its fidelity affects lifespan.

INTRODUCTION

The production of properly made and folded proteins is crucial for normal cell function and organismal survival. Conversely, misfolded proteins can lead to a number of common and serious diseases, including several neurodegenerative disorders [1].

With respect to protein production, maintaining accuracy during protein synthesis (mRNA translation) is crucial for the faithful decoding of genetic information to generate fully functional proteins. However, mRNA translation has a higher intrinsic error rate than DNA polymerase [2]. Misincorporated amino acids are subject to "editing" in bacteria [3], but eukaryotes do not appear to have an analogous function for editing after decoding [4]. It has been shown that in mammals, as an evolutionary phenomenon, high levels of translational accuracy correlate positively with longer lifespan [5, 6]. It therefore follows that cells require mechanisms to optimize the accuracy of protein synthesis without compromising the efficiency of protein production. Interestingly, one of the major pathways that modulates accelerated aging in eukaryotic organisms, target of rapamycin complex 1 (TORC1) signaling [7], also activates protein synthesis and other anabolic processes [8]. Recently, Conn and Qian [9] showed that active mammalian (m)TORC1 signaling impairs translational accuracy (also termed "fidelity"). Errors in amino acylation of tRNAs and codon decoding can each affect accuracy. Given that >99% of amino acids are incorporated during elongation, the vast majority of translation accuracy errors are made during this stage of translation [10].

During mRNA translation, aminoacyl-tRNAs are recruited into the ribosomal A site by eukaryotic elongation factor 1A (eEF1A). After achieving an appropriate codon:anticodon match, the corresponding amino acid is added to the growing polypeptide by forming a peptide bond and concomitant transfer of the nascent chain to the A site tRNA. There is no known connection between mTORC1 signaling and regulation of this step in elongation.

The ribosome then undergoes translocation, whereby it moves the equivalent of one codon along the mRNA, thereby bringing the peptidyl-tRNA into the P site and the next codon into the

Table 1. List of Specific Terms Used in This Study

Term	Meaning
(h)MaxCFluc	fastest firefly luciferase constructs according to human decoding time
StaCFluc	original wild-type "standard" firefly luciferase
(h)MinCFluc	slowest firefly luciferase constructs according to human decoding time
R218S	arginine position 218 to serine missense mutation
STOP	leucine position 210 to STOP codon mutation
PEST	a motif that causes the destabilization and rapid degradation of newly synthesized firefly luciferase ($t_{1/2} \approx 2$ h)

now-vacant A site. This step requires a second elongation factor, eEF2, whose activity is inhibited by phosphorylation, which is in turn controlled by mTORC1 signaling [11].

The phosphorylation of eEF2 on Thr56 decreases its affinity for the ribosome, thereby inactivating it [12]. eEF2 is phosphorylated by a dedicated protein kinase, eEF2 kinase (eEF2K), which belongs to the atypical α-kinase family and is subject to tight regulation [13]. For example, it is inactivated by anabolic and mitogenic signaling pathways such as mTORC1 and the classical extracellular signal-regulated kinase (ERK) MAP kinase pathway [14]. Thus, activation of these anabolic or mitogenic signaling pathways turns off eEF2K, ensuring that eEF2 and elongation are active. Consistent with this, when initiating ribosomes are stalled using harringtonine, TSC2 null cells (in which mTORC1 signaling is constitutively activated [15]) exhibit earlier ribosomal runoff, indicating a faster rate of translation elongation (reflecting disinhibition of eEF2), whereas rapamycin—which inhibits mTORC1—slows down elongation [11]. Conversely, eEF2K is activated by Ca^{2+} ions at low pH and under various stress conditions [16].

Given that mTORC1 controls the activity of eEF2K and thus elongation, we asked whether the effects of mTORC1 signaling on fidelity involve the regulation of eEF2 by eEF2K. Surprisingly, given that eEF2 is not involved in the step of elongation where cognate aminoacyl-tRNAs are selected, we find activation of eEF2K enhances translational fidelity, indicating that its activity nonetheless governs the accuracy of elongation.

Inhibition of (m)TORC1 as well as controlled nutritional restriction are known to extend lifespan in a variety of organisms [7]. We have therefore also explored the impact of this regulatory system on lifespan; deletion of the eEF2K ortholog reduces the lifespan of *C. elegans*. Taken together, our data reveal a crucial role for eEF2K in reducing errors in translation, and that reducing translation elongation rates improves translation fidelity and extends lifespan.

RESULTS

The Speed of Translation Elongation Dictates Translation Accuracy

The rate of translation elongation can be affected by the codon composition of the translated region of mRNAs; because some codons are used less often than others and hence there are fewer tRNAs with the corresponding anticodon, it takes longer to achieve a codon:anticodon match for such codons. This can therefore slow down the decoding of the mRNA [17]. Previously, constructs were created encoding firefly luciferase (Fluc; see Table 1 for a list of specific terms used in this study) using the slowest (yeast MinCFluc) and fastest (yeast MaxCFluc) possible codons [18]. Similarly, and to assess whether codon usage modulates synthesis rates in human cells, we made the slowest (human [h]MinCFluc) and fastest (hMaxCFluc) constructs according to predicted human decoding times (Figures 1A and S1A–S1J) in a vector that also contains a cistron encoding Renilla luciferase (Rluc); Rluc activity levels allow the Fluc data to be normalized to control for factors such as transfection efficiency or overall translational activity. All data are therefore given as "relative Fluc activity," i.e., Fluc/Rluc ratio as a % of the corresponding control conditions. We named the original wild-type "standard" Fluc "StaCFluc." hMaxCFluc produced the highest amount of active Fluc protein, whereas hMinCFluc produced much less (Figures 1B, S1I, and S1J), showing that codon composition strongly affects the overall efficiency of protein expression and thereby demonstrating that elongation rates limit the overall rate of translation of this mRNA.

In yeast, bacterial [19], and mammalian [9] cells, faster elongation rates compromise the accuracy of codon:anticodon recognition, although it has recently been reported that rates of translation elongation do not correlate with translation fidelity in yeast [20, 21]. The above constructs allow us to assess the extent to which the rate of elongation affects the accuracy (fidelity) of mRNA translation, and explore what factors affect this. To do this, we created two Fluc reporter missense mutants for use in mammalian cells. In the first, the arginine codon (AGA) at position 218 was changed to a serine codon (AGT), yielding the "Fluc[R218S]" vectors. Because Arg218 is a key residue for binding of substrate to luciferase [22], correct decoding at this position generates catalytically inactive protein. The level of active luciferase (in which this codon has actually been misread as encoding arginine) therefore serves as an indicator of misreading of the serine codon to incorporate arginine, i.e., lack of fidelity during elongation [23]. In the second variant, the leucine codon (CTT) at position 210 of the corresponding amino acid sequence was replaced by a stop codon (TGA, yielding the Fluc[STOP] vector), allowing us to detect readthrough errors during translation [23], i.e., another failure in its accuracy. Because changes in steady-state protein levels could, in principle, also result from altered rates of protein degradation, we made the same mutations in a StaCFluc reporter that encodes Fluc followed by a PEST motif (SSGTRHGFPPEVEEQAAGTLPMSCSQESGMD RHPAACASARINV). This motif causes the destabilization and rapid degradation of newly synthesized Fluc ($t_{1/2} \approx 2$ h) [24] (vectors termed Fluc[R218S-PEST] and Fluc[STOP-PEST], respectively; see Figure S1E). This accelerates the turnover of Fluc, allowing us to more accurately assess new Fluc protein production without interference from already-existing enzyme present at the start of the treatment.

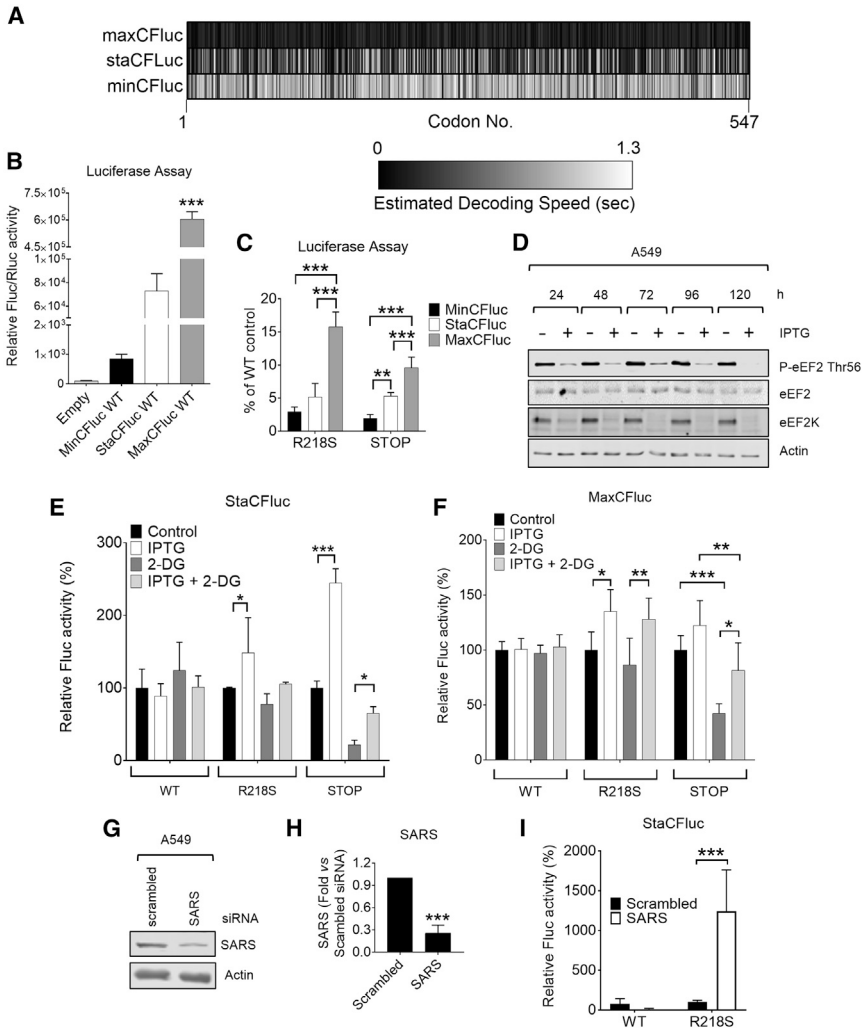

Figure 1. Accelerated Translation Speed Correlates with a Reduction in Translation Fidelity

(A) The heatmap illustrates the calculated decoding speed of the designed Min/Sta/MaxCFluc constructs (a color bar is shown below for reference).

(B) HEK293 cells were transfected with empty pICtest2 or pICtest2 vectors encoding Min/Sta/MaxCFluc. After 48 h, Fluc activity was quantified using luciferase assay.

(C) HEK293 cells were transfected with the MinCFluc WT, R218S, or STOP; StaCFluc WT, R218S, or STOP; or MaxCFluc WT, R218S, or STOP constructs. After 48 h, relative Fluc activity was then analyzed using luciferase assay. The relative Fluc expression levels when using R218S or STOP constructs were then normalized and presented as % of WT control.

(D) A549 cells were treated with 1 μM IPTG for up to 120 h (5 days) to induce the expression of an shRNA against *EEF2K*.

(E and F) IPTG (1 μM) was added to A549 cells 5 days before the experiment to induce expression of an shRNA against *EEF2K*. A549 cells were transfected with StaCFluc (E)/MaxCFluc (F) WT, R218S, or STOP constructs, and cells were then cultured in DMEM containing low glucose (5.5 mM) for 1 h, before treatment with 2-DG (10 mM) for 16 h. Fluc activity was quantified using luciferase assay and normalized to mock-treated controls. Results are given as means ± SD; n = 3 independent experiments, each performed in triplicate.

(G) A549 cells were transfected with scrambled or SARS siRNA. After 72 h, they were lysed, and samples were subjected to immunoblotting analysis with the indicated antibodies.

(H) Quantification of SARS from (G).

(I) A549 cells were transfected with scrambled or SARS siRNAs. After 24 h, the cells were transfected with StaCFluc WT or R218S vectors. 48 h later, luciferase activity was quantified. Results are given as means ± SD; n = 4 independent experiments, each performed in triplicate.

Results are given as means ± SD. *$0.01 \leq p < 0.05$, **$0.001 \leq p < 0.01$, ***$p < 0.001$, as determined by two-way ANOVA followed by Dunnett's test (A) or Tukey's test (C); n = 4 (B and C). See also Figures S1 and S3–S5.

Importantly, we observed the highest levels of these translation errors (higher luciferase activity) in HEK293 cells transfected with the hMaxCFluc mutants, whereas the lowest levels of FLuc, and therefore of errors, were seen in cells transfected with the hMinCFluc mutants (Figure 1C; note that data are always compared to the differing yields of active luciferase for the corresponding parent Min, Sta, or Max vectors). These results show that faster translation elongation leads to impaired translational fidelity.

eEF2K Promotes Translational Fidelity

Because eEF2K regulates the rate of elongation, we wished to explore its role in modulating translational fidelity. As noted above, eEF2K is activated under diverse stress conditions [25–29]. Using A549 (human lung adenocarcinoma) cells, we first studied the effects of (1) energy deprivation, mimicked by treating cells with 2-deoxyglucose (2-DG), a glucose analog that can be phosphorylated by hexokinase but cannot be metabolized through glycolysis; consequently, it depletes cells of ATP; (2) nutrient deprivation (cells were transferred to Dulbecco's [D-] PBS); and (3) extracellular acidosis, which activates eEF2K [16]. We also treated cells (4) with the mTOR inhibitor AZD8055 [30], which alleviates inhibitory inputs into eEF2K (Figures S1K–S1S and S2A–S2D). As expected, each of these conditions inhibited mTORC1 signaling, as shown by decreased rpS6 phosphorylation (downstream of mTORC1), and evoked activation of eEF2K, as indicated by increased eEF2 phosphorylation (Figures S1K–S1S and S2A–S2D). Notably, in A549 cells, 2-DG treatment rapidly induced the phosphorylation of eEF2 (within 30 min), which persisted for at least 16 h (Figures S2A–S2D).

To test the role of eEF2K in translational accuracy, we made use of A549 or HCT116 cells that inducibly express a short hairpin (sh)RNA that targets the *EEF2K* mRNA (Figures 1D–1F and S1K–S1N) [28]. We transfected them with vectors for wild-type (WT) or mutant StaCFluc. In some cases, cells were treated with isopropyl β-D-1-thiogalactopyranoside (IPTG) to induce the

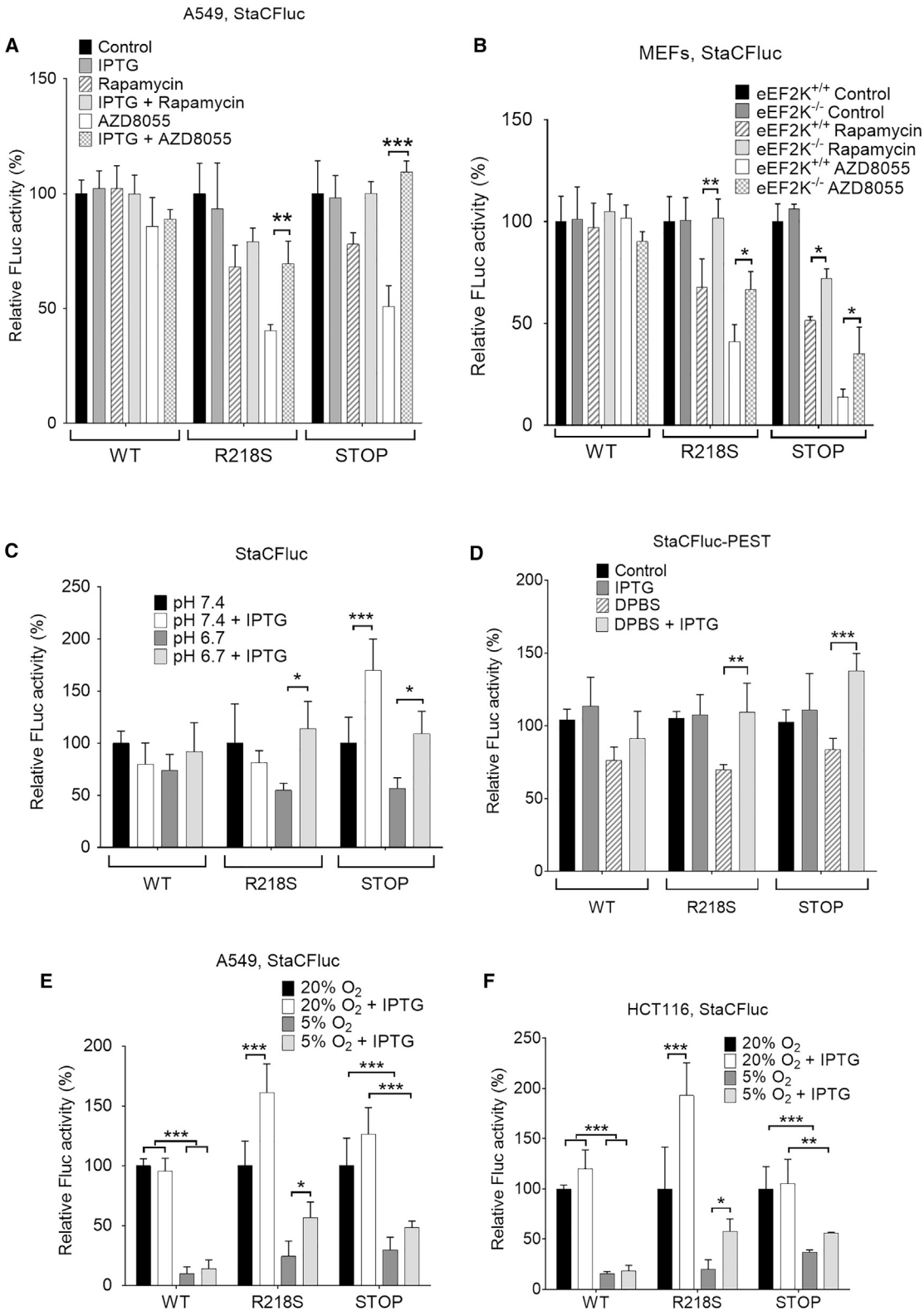

Figure 2. eEF2K Activation Enhances Translation Fidelity

(A) A549 cells were transfected with StaCFluc WT, R218S, or STOP constructs. After 24 h, cells were treated with vehicle (DMSO, as a control), rapamycin (200 nM), or AZD8055 (1 μM) for 16 h. After 16 h, Fluc activity was determined using luciferase assay.

(legend continued on next page)

shRNA against *EEF2K* (1–4). Cells were then cultured for 16 h in the presence or absence of 2-DG. Knocking down eEF2K by inducible shRNA did not affect the Fluc/Rluc activity ratio from the Min/Sta/MaxCFluc[WT] or StaCFluc[WT-PEST] vectors (Figures 1E, 1F, S2E, S3, and S4). However, knockdown of eEF2K did increase expression of active StaCFluc from the StaCFluc [R218S-PEST] and StaCFluc[STOP-PEST] vectors (Figures S3C–S3E), as well as Min/Sta/MaxCFluc[R218S] and Min/Sta/MaxCFluc[STOP] (Figures 1D–1F and S3) either under basal conditions (cells cultured in DMEM containing low glucose [5.5 mM]) or when cells were treated with 2-DG.

We also used CRISPR/Cas9 genome editing to generate eEF2K knockout (KO) MDA-MB-231 (human breast cancer) cells. Whereas incubation in 2-DG slowly increased p-eEF2 levels in WT cells (Figure S5A), no eEF2 phosphorylation was seen in KO cells (Figure S5B). We observed an increase in the expression of active StaCFluc from StaCFluc[R218S]-transfected eEF2K-KO cells as compared to control cells (Figure S5C), similar to our observations for A549 and HCT116 cells where *EEF2K* was knocked down by inducible shRNA (Figures 1D–1F and S3). *Fluc* mRNA abundance (Figures S4A–S4D) as well as Fluc protein expression levels (Figures S4E–S4K) were very similar in WT and IPTG-treated A549 cells and in eEF2K$^{+/+}$ and eEF2K$^{-/-}$ mouse embryonic fibroblasts (MEFs); thus, the differences in Fluc activity observed (Figures 1, S2E, and S3) were not due to a difference in transfection, transcription, or translation efficiency. Levels of total Fluc from the WT or R218S vectors were very similar, indicating that the differences in activity reflect mistranslation in the case of the latter (Figure S4E). (Note that MinCFluc [Figure S1I] and Fluc[STOP] [Figure S4E] were not detected by the Fluc antibody, in the former case as levels were too low and in the latter probably because either the epitope lies after the stop codon or the truncated Fluc is rapidly degraded.)

Aminoacyl-tRNA synthetases (aaRSs) play a crucial role in protein synthesis and in maintaining its fidelity by generating correctly charged tRNAs. Errors during elongation may arise from competition of cognate and near-cognate aminoacyl-tRNAs at the ribosomal A site; therefore, lower levels of the cognate aminoacyl-tRNA are expected to give near-cognate aminoacyl-tRNAs a higher chance of being accepted at a given codon [31]. Consistent with this, and as expected from the nature of the mutation in this vector, expression of StaCFluc [R218S] was greatly enhanced in cells where expression of the seryl aminoacyl-tRNA synthetases (SARS) was knocked down by small interfering RNA (siRNA) (Figures 1G–1I). The observed magnitude of the change may be an underestimate, because SARS knockdown led to a reduction in the expression of StaCFluc[WT].

Inhibition of mTORC1 Signaling Improves Translation Fidelity through the Activation of eEF2K

Active mTORC1 signaling increases global protein synthesis but impairs translational fidelity [9]. Because mTORC1 is an upstream negative regulator of eEF2K [16], we asked whether eEF2K mediates the effect of mTORC1 on translational fidelity. For this purpose, we incubated A549 cells (Figures 2A, S1K, and S1M) as well as eEF2K$^{+/+}$ and eEF2K$^{-/-}$ MEFs (Figures 2B, S1L, and S1N) in the presence or absence of rapamycin or AZD8055 [30]. As expected, rapamycin or AZD8055 treatment abolished the phosphorylation of rpS6 at Ser240/Ser244, indicating mTORC1 was inhibited, and increased the phosphorylation of eEF2 at Thr56 (Figures S1K–S1N). Genetic deletion of eEF2K totally blocked phosphorylation of eEF2 (Figure S1N).

Rapamycin or AZD8055 treatment reduced expression of active StaCFluc from StaCFluc/StaCFluc-PEST [R218S] and [STOP] vectors but not from the WT vector, indicating lower rates of misreading or termination readthrough errors. Consistently, knocking down eEF2K using inducible shRNA in A549 cells (Figures 2A and S5D) or KO of eEF2K in MEFs (Figure 2B) significantly attenuated the ability of mTOR inhibitors to decrease error rates. Thus, the ability of mTORC1 signaling to modulate error rates requires eEF2K, an effector of mTORC1 signaling. The data show that mTORC1 regulates translation fidelity by affecting the rate of translation elongation via eEF2K, thus providing a clear molecular mechanism to explain the findings of Conn and Qian regarding the impact of mTORC1 signaling on translation fidelity [9].

eEF2K Is a General Modulator of Translation Fidelity

We also wished to test whether eEF2K is involved in maintaining the quality of translation under other conditions. We therefore incubated A549 cells, which had been transfected with vectors for StaCFluc[WT] or mutants, under stress conditions known to activate eEF2K, i.e., incubation in medium buffered at low pH (pH 6.7; Figures 2C, S1O, and S1P), in DPBS (which lacks amino acids; Figures 2D, S1Q, and S1R), or under hypoxia (Figures 2E, 2F, and S1S). All these treatments inhibited signaling through mTORC1, as shown by the decreased rpS6 phosphorylation and increased electrophoretic mobility of 4E-BP1 (reflecting its dephosphorylation) (Figures S1I–S1S). Phosphorylation of eIF2α, a key regulator of translation initiation, was not affected, although it was induced by cycloheximide (used as a positive control for the P-eIF2α antibody; Figure S5E).

Inducing the shRNA reduced eEF2K levels and attenuated eEF2 phosphorylation (Figures 2E, 2F, and S1I–S1S). Incubation in DPBS modestly decreased StaCFluc-PEST[WT] (Figure 2D), whereas hypoxia (5% oxygen) greatly reduced StaCFluc[WT]

(B) eEF2K$^{+/+}$ and eEF2K$^{-/-}$ MEFs were transfected with StaCFluc WT, R218S, or STOP, and then incubated with vehicle (DMSO), rapamycin (200 nM), or AZD8055 (1 μM). After 16 h, Fluc activity was determined using luciferase assay.

(C) A549 cells were transfected with StaCFluc WT, R218S, or STOP constructs. 24 h later, cells were incubated in pH (7.4 or 6.7) buffered medium for 16 h, before luciferase assay analysis.

(D) A549 cells were transfected with Fluc-PEST WT, R218S, or STOP constructs, followed by incubation in growth medium or DPBS for 3 h, before luciferase assay analysis.

(E and F) A549 (E) or HCT116 (F) cells were transfected with StaCFluc WT, R218S, or STOP constructs. After 24 h, they were incubated in 20% or 5% O_2 for 16 h, before luciferase assay.

For experiments performed in A549 (A and C–E) and HCT116 (F) cells, IPTG (1 μM) was added to cells 5 days before StaCFluc transfection to induce the expression of shRNA against *EEF2K*. Fluc activity is expressed as means ± SD; n = 4 (A–D) or 3 (E and F) independent experiments performed in triplicate. See also Figures S1, S2, and S4–S6.

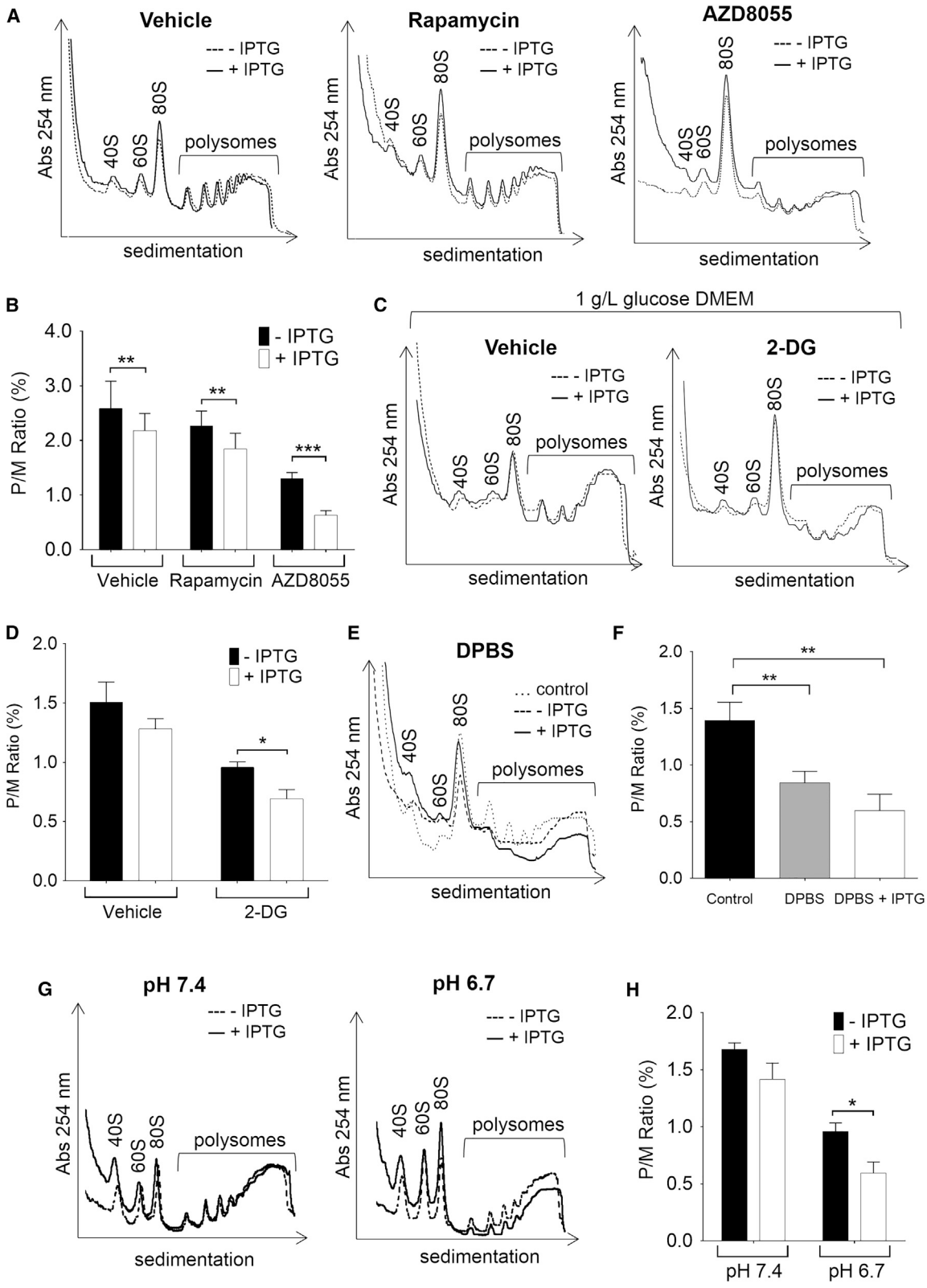

Figure 3. eEF2K Knockdown Reduces Polysome/Monosome Ratio in A549 Cells

(A) Polysome profile analysis of lysates from A549 cells treated with vehicle (DMSO) control, rapamycin (200 nM), or AZD8055 (1 μM) for 16 h.

(B) Polysome/monosome (P/M) ratio quantification of data in (A).

(legend continued on next page)

levels (Figures 2E and 2F). Cells cultured in medium buffered at low pH (6.7), in DPBS, or under hypoxia exhibited reduced levels of active Fluc from the StaCFluc, StaCFluc-PEST R218S, or STOP vectors (Figures 2C–2F), indicating enhanced translational accuracy. Although knockdown of eEF2K did not affect the expression of StaCFluc/StaCFluc-PEST[WT], it did increase levels of active (mistranslated) StaCFluc/StaCFluc-PEST R218S under these conditions (Figures 2C–2F and S5F). These data provide further evidence that eEF2K serves as a "guardian" of translation fidelity under diverse stress conditions.

Slower Elongation, Not Lower Overall Protein Synthesis, Enhances Fidelity

The treatment of cells with 2-DG, AZD8055, DPBS, or low pH decreased global protein synthesis. Although knocking down eEF2K did not affect overall protein synthesis rates under any of the conditions tested (Figures S5G–S5J), it did increase the proportion of translationally inactive monosomal fractions concomitant with a decrease in translationally active polysomal fractions, as analyzed on sucrose density gradients (Figure 3). This presumably reflects faster rates of elongation in the knockdown cells (as fewer ribosomes are engaged in polysomes at any given time, due to ribosomal "run-off"). Hence, the positive effect of eEF2K on translation fidelity reflects slower translation elongation rather than lower overall rates of protein synthesis.

The AMPK Pathway Is Crucial for Maintaining Translation Fidelity

Stress conditions can evoke activation of eEF2K via the AMPK. Genetic KO of AMPK completely (2-DG; Figure 4A) or partially (AZD8055, DPBS, low pH; Figure 4B) prevented increased phosphorylation of eEF2, indicating that AMPK plays a role in mediating these effects. In line with our previous studies [28, 29], we also observed a reduction in levels of eEF2K protein in AMPK null MEFs (Figures 4A and 4B); this may well also contribute to the lower eEF2 phosphorylation seen in these cells.

Importantly, compared to WT MEFs, AMPK null MEFs transfected with the Fluc vector exhibited higher levels of Fluc activity from the StaCFluc[R218S] and StaCluc[STOP] but not from the StaCFluc[WT] vectors (Figure 4C), illustrating that AMPK helps ensure translational accuracy under stress conditions. Given that AMPK activates eEF2K, and the above data linking eEF2K to translational accuracy, these effects are likely to be mediated via activation of eEF2K and concomitant inhibition of eEF2.

For experiments where cells were treated with 2-DG, they were transferred into medium containing lower glucose levels (5.5 mM). Even without 2-DG, this resulted in increased p-eEF2 levels (Figures S3 and S4). This likely explains why we observed an increase in Fluc activity in Fluc[R218S]/Fluc[STOP]-transfected or eEF2K knockdown A549 or HCT116 cells (Figures 1E, S2E, and S3), as well as in AMPK$^{-/-}$ MEFs (Figure 4C), when compared to the corresponding control cells.

Reducing Cellular Levels of eEF2 Also Improves the Fidelity of Translation

Our data indicate that stimulation of eEF2K, and thus lower eEF2 activity, promotes translational accuracy. It follows that reducing eEF2 protein levels should also improve fidelity. Accordingly, A549 cells were transfected with siRNA against eEF2 and, 24 h later, with the vectors encoding Fluc or mutants. After a further 48 h, by which time eEF2 levels had been reduced substantially (Figure 4D), luciferase activity was measured. Knockdown of eEF2 decreased the levels of active luciferase from the StaCFluc [R218S] and StaCFluc[STOP] vectors but had no effect on WT StaCFluc expression (Figure 4E). Taken together, these data indicate that the AMPK-eEF2K-eEF2 pathway is crucial for translation quality control when cells are subjected to stress conditions.

eEF2K Modulates Start Codon Selection during Translation Initiation

The process of start-site selection in eukaryotes differs fundamentally from aminoacyl-tRNA choice during elongation; in particular, during initiation, the 40S subunit (with its associated factors) is already equipped with the initiator methionyl-tRNA and is seeking the correct codon, whereas in elongation the converse is true: a correct match has to be achieved between the codon already in the A site and the relevant aminoacyl-tRNA. Chu et al. [18] reported that in yeast, when rare (infrequently used) codons are positioned immediately after the translation start codon, the impaired speed of translation elongation restricts the "liberation" of the 40S ribosome from the start codon and hence loading of the next 40S subunit. Under these circumstances, translation elongation can affect initiation. However, it was not known whether this also applies in mammalian cells. Because eEF2K regulates the rate of elongation, we asked whether eEF2K affected the stringency of translation start-site selection.

We previously [32] developed "pICtest2" dual-luciferase reporters with non-AUG start codons as well as an inferior Kozak consensus (non-optimal initiation [start]-site context). To test the effect of eEF2K on start-site recognition, we selected two near-cognate non-AUG start codon variants (GUG and CUG).

We first compared the relative expression levels of luciferase expressed from these plasmids in A549 cells. Non-AUG start codon plasmids exhibited 7.7% (GUG) or 17.3% (CUG) of Fluc activity compared to the WT Fluc (AUG start codon with optimal Kozak consensus; Figure 5A).

Treating the cells with 2-DG to increase eEF2 phosphorylation tended to reduce the expression of Fluc. Knocking down eEF2K significantly increased the expression of active Fluc from GUG or CUG as start codons but did not affect expression of Fluc with

(C) A549 cells were cultured under low-glucose (5.5 mM) DMEM for 1 h before the addition of 2-DG (10 μM) for 16 h. Cells were then subjected to polysome profile analysis.
(D) Polysome/monosome ratio (polysome/monosome) quantification of (C).
(E) A549 cells were cultured either in growth media or DPBS for 3 h before polysome profile analysis.
(F) Polysome/monosome ratio (polysome/monosome) quantification of (E).
(G) A549 cells were cultured in pH (7.4 or 6.7) buffered medium for 16 h before polysome profile analysis.
(H) Polysome/monosome ratio (polysome/monosome) quantification of (G).
For all experiments, IPTG (1 μM) was added to A549 cells 5 days before experiments to induce the expression of shRNA against *EEF2K*.

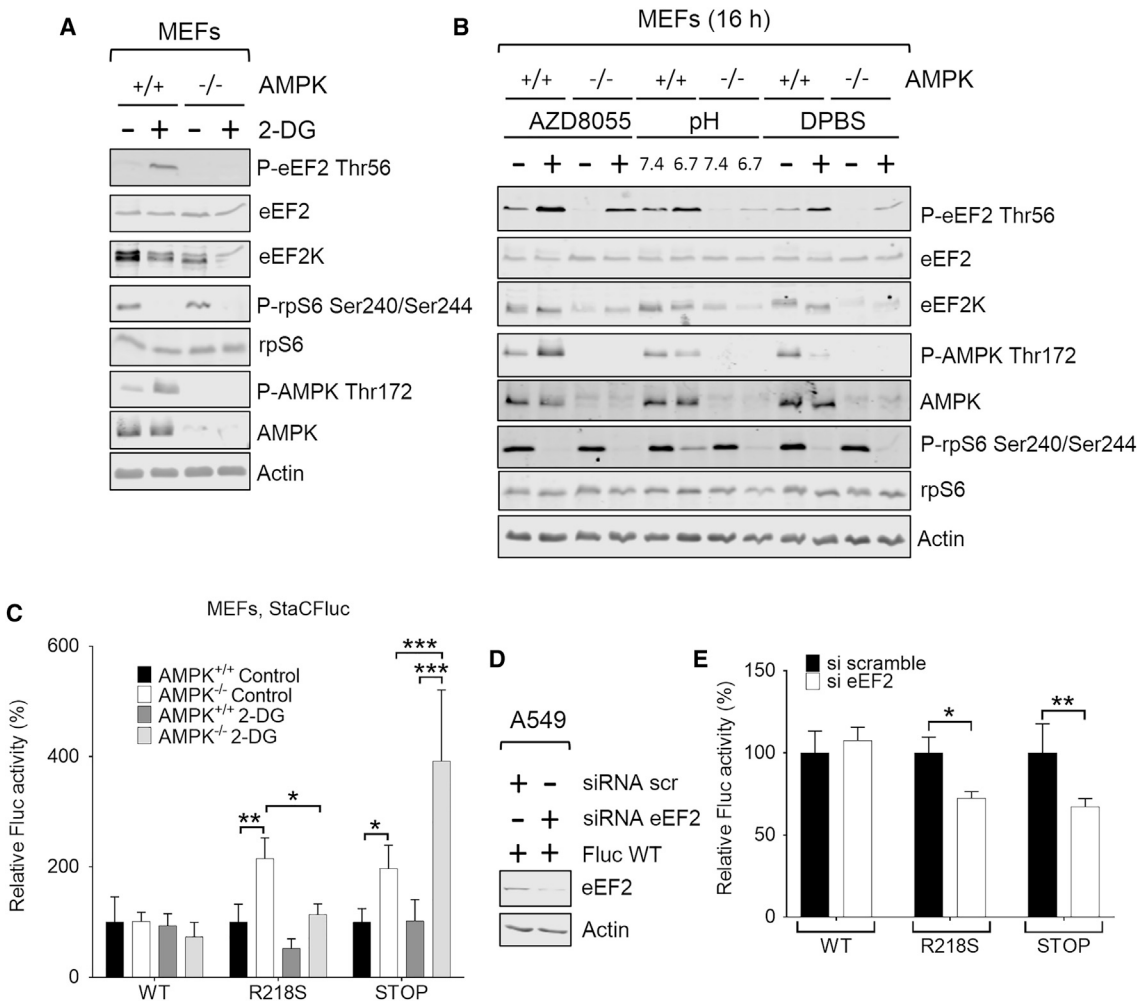

Figure 4. AMPK Helps to Promote Translation Fidelity

(A) AMPK$^{+/+}$ and AMPK$^{-/-}$ MEFs were pre-incubated in low-glucose (5.5 mM) DMEM for 1 h, before treatment with 2-DG (10 mM) for 16 h.

(B) AMPK$^{+/+}$ and AMPK$^{-/-}$ MEFs were cultured for 3 h with 1 μM AZD8055 or vehicle (DMSO), or in medium buffered at pH 7.4 or 6.7 for 16 h, or growth medium (as control) or DPBS. Cells were then lysed and lysates were subjected to immunoblotting analysis with the indicated antibodies.

(C) AMPK$^{+/+}$ and AMPK$^{-/-}$ MEFs were transfected with StaCFluc WT, R218S, or STOP constructs. After 24 h, cells were then placed in low-glucose (5.5 mM) DMEM for 1 h, before being treated with 2-DG (10 mM) for 16 h. Fluc activity was measured and normalized to vehicle-treated control.

(D) A549 cells were transfected with scrambled siRNA or siRNA against *EEF2* for 24 h; cells were then transfected with WT/R218S/STOP StaCFluc. After 48 h, cells were lysed followed by SDS-PAGE/western blotting analysis.

(E) Cells were treated as in (D), and luciferase activity was measured.

Results are given as means ± SD; n = 4 independent experiments performed in duplicate. *$0.01 \leq p < 0.05$, **$0.001 \leq p < 0.01$, ***$p < 0.001$, as obtained by two-way ANOVA.

AUG as start codon (Figure 5B). This implies that increased phosphorylation of eEF2, and thus slower elongation, also aids the fidelity of start codon recognition, by augmenting the ability of ribosomes to distinguish between AUG and near-cognate start codons (Figure 5C).

eEF2K Does Not Affect Chaperone or Proteasome Activity

It was important to assess whether changes in chaperone or proteasome activity contributed to the increase in active Fluc that we observe when knocking down eEF2K. *In vitro* Fluc-refolding assays revealed that there was a slight decrease in refolding ability when denatured recombinant Fluc was incubated with lysates from eEF2K knockdown A549 cells that had been pre-treated with 2-DG, pH 6.7 medium, or AZD8055 (Figures S5K–S5N) as compared to lysates from control cells with normal eEF2K levels. The reduced refolding capacity might reflect higher levels of client misfolded proteins resulting from impaired translation fidelity in the knockdown cells. The rise in active Fluc levels upon eEF2K knockdown cannot therefore be explained by lower protein folding or chaperone capacity; indeed, these data may indicate that the measured effects of eEF2K to promote translation fidelity are a slight underestimate.

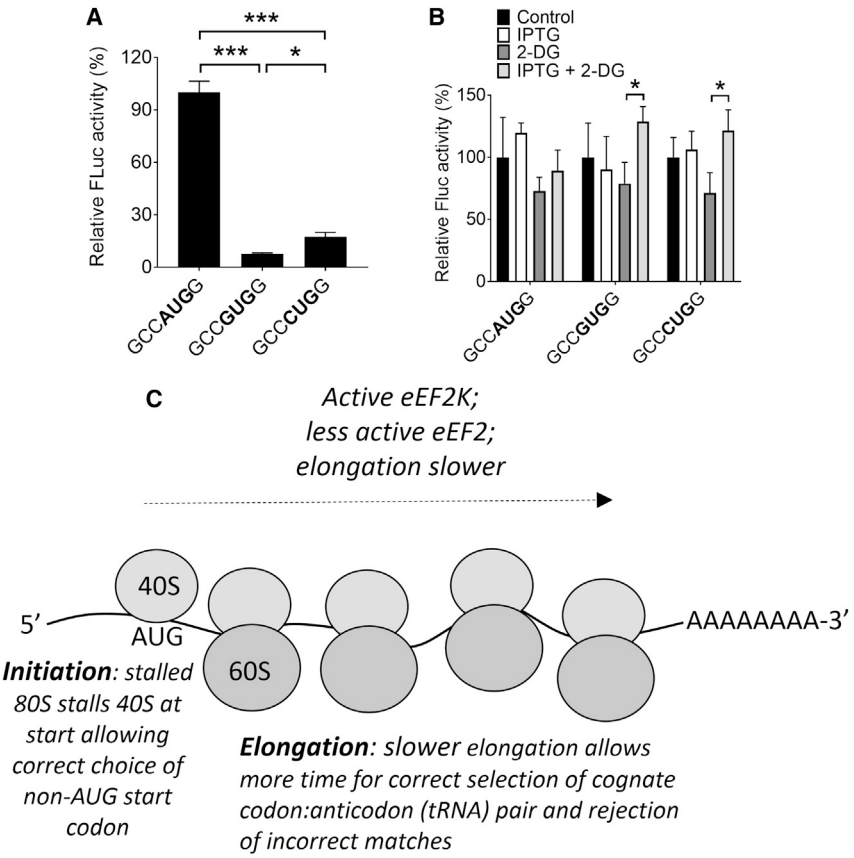

Figure 5. eEF2K Stimulation Increases the Stringency of Initiation Codon Selection

(A) A549 cells were transfected with pICtest2 vectors encoding StaCFluc with different start codons (previously reported in [1]; sequences are indicated). Fluc activity was then measured, and is expressed as percentage of control (GCCAUGG) (means ± SD; n = 4 independent experiments conducted in triplicate). 0.01 ≤ *p < 0.05, ***p < 0.001, as obtained by one-way ANOVA followed by Dunnett's test.

(B) A549 cells were transfected with pICtest2 reporter vectors as in (A), and after 48 h were treated with 2-DG as in Figures 1D–1F. Fluc activity was measured and is expressed as percentage of control (means ± SD; n = 4 independent experiments, each performed in triplicate).

(C) Schematic representation of how slow elongation speed favors the correct selection of the start codon as well as of the cognate codon:anticodon (tRNA) pair.

To study the effect of altered eEF2K levels on the ubiquitin-proteasome system, we treated A549 and HCT116 cells with the proteasome inhibitor MG132. Increasing concentrations of MG132 evoked phosphorylation of eEF2, indicating activation of eEF2K, in parallel with an increase in polyubiquitinated proteins (Figures S6A–S6C). Knocking down eEF2K did not lead to obvious changes in polyubiquitin signals or WT StaCFluc expression in A549 or HCT116 cells (Figures S6B and S6C). We also applied a cell-based proteasome assay to measure its chymotrypsin-like activity in these cells (Figures S6D–S6G). We observed decreased proteasome activity in 2-DG-treated A549 cells (Figure S6D) and increased proteasome activity in A549 cells that had been incubated in DPBS (Figure S6G). However, under no conditions tested did knockdown of eEF2K affect proteasome activity (Figures S6D–S6G).

Taken together, these data imply that the increases in active Fluc seen in the absence of eEF2K are not due to changes in protein folding or proteasome activity.

Aminoacyl-tRNA Synthetase Orthologs and the eEF2K Ortholog efk1 Control Lifespan in *C. elegans*

mRNA translation accuracy strongly correlates with lifespan of organisms during evolution [5, 6]. Mammals with high rates of translation fidelity live longer than those with high levels of translation inaccuracy [6]. We argued that inadequate levels of aminoacyl-tRNA synthetases are expected to impair fidelity by limiting the availability of specific aminoacyl-tRNAs, leading to misincorporation of amino acids at the codons normally recognized by those charged tRNAs (due to use of a near-cognate but incorrect aminoacyl-tRNA). Similar findings were recently reported in yeast [20]. To test this, we knocked down selected aminoacyl-tRNA synthetases in *C. elegans*, a short-lived nematode worm that is widely used to study the control of lifespan. (Because, unlike eEF2K, these are essential genes, they cannot be completely knocked out.) Depletion of the leucyl- (*lrs-1*), arginyl- (*rrs-1*), asparaginyl- (*nrs-1*), or methionyl-tRNA (*mrs-1*) synthetases significantly decreased lifespan when worms were maintained at 25°C on normal food, implying that impaired translation fidelity does indeed shorten lifespan (Figure 6A). *Drosophila* is a widely used and tractable model for studying lifespan, but lacks an ortholog of eEF2K. We found that when leucyl-tRNA synthetase (LeuRS) was knocked down during adulthood in *Drosophila*, there was a marked reduction in lifespan (Figures S7A and S7B), analogous to our findings in *C. elegans* (Figure 6A).

C. elegans has an ortholog of eEF2K; its target residue in eEF2 and the adjacent sequence are conserved in *C. elegans* eEF2 [27]. As expected, caloric restriction (achieved by using heat-killed [HK] *E. coli* as food) extended the lifespan of WT N2 worms (Figure 6B). *efk-1* KO worms (*0k3609*) (previously characterized in [33]) had only a slightly reduced lifespan on normal diet but, importantly, showed no extension upon caloric restriction (Figure 6B). These data indicate that eEF2K is required for lifespan extension induced by nutrient restriction. Interestingly, depletion of *mrs*-1 but not of other aminoacyl-tRNA synthetases (*lrs-1*, *kars-1*, and *nrs-1*) further reduced the lifespan of *efk-1* KO worms under normal (OP50) feeding (Figure 6C). This likely reflects the fact that the latter three enzymes are only required for elongation, which is controlled by eEF2K, whereas *mrs-1* is also needed for translation initiation.

It has previously been shown that inhibition of TOR in *C. elegans* extends lifespan [34]. Here, we observed that rapamycin-treated *efk-1* KO worms still outlived rapamycin-treated

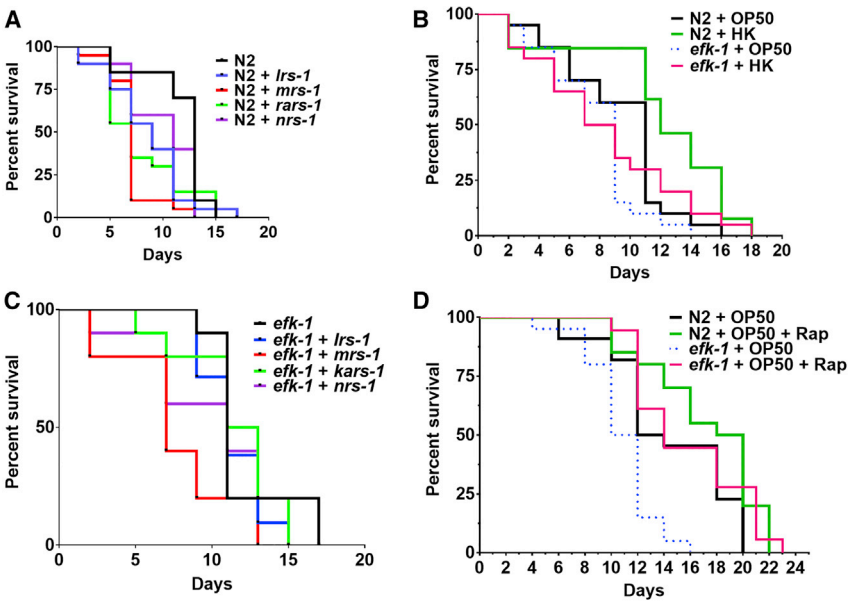

Figure 6. Factors that Increase Translation Fidelity Affect Lifespan in *C. elegans*

(A) Lifespan of WT (N2), *lrs-1*, *mrs-1*, and *rrs-1* knockdown worms under standard growth conditions. Mean survival: N2, 13 days; N2/*lrs-1*, 9 days; N2/*mrs-1*, 7 days; N2/*rrs-1*, 7 days; N2/*nrs-1*, 11 days. N2 versus N2/*mrs-1*: p = 0.0075; N2 versus N2/*lrs-1*: p = 0.0023; N2 versus N2/*rrs-1*: p = 0.0075; N2 versus N2/nrs-1: p = 0.0291.

(B) The lifespan of N2 and efk-1 knockout worms when fed with normal food or under caloric restriction (fed with heat-killed [HK] *E. coli*). Mean survival: N2/OP50 (fed normally with *E. coli* OP50), 11 days; N2/HK, 12 days; *efk-1*/OP50, 9 days; *efk-1*/HK, 9 days. N2/OP50 versus N2/HK: p = 0.0146; N2/HK versus *efk-1*/ HK: p = 0.0358; N2/OP50 versus *efk-1*/OP50: p = 0.0006.

(C) Lifespan of *efk-1*, *efk-1* + *lrs-1*, *efk-1* + *mrs-1*, *efk-1* + *nrs-1*, and *efk-1* + *kars-1* knockdown worms under standard growth conditions. Mean survival: *efk-1*, 11 days; *efk-1* + *lrs-1*, 11 days; *efk-1* + *mrs-1*, 7 days; *efk-1* + *nrs-1*, 11 days; *efk-1* + *kars-1*, 12 days. *efk-1* versus *efk-1* + *mrs-1*: p = 0.0006.

(D) The lifespan of N2 and *efk-1* worms when fed with normal food (OP50) containing 100 μM rapamycin (Rap) where indicated. Mean survival: N2/OP50, 12 days; N2/OP50/Rap, 18 days; *efk-1*/OP50, 10 days; *efk-1*/OP50/Rap, 14 days. *efk-1*/OP50 versus *efk-1*/OP50 + Rap: p < 0.0001; N2/OP50 versus *efk-1*/OP50: p = 0.0006.

See also Figure S7.

WT worms (Figure 6D), implying that *efk-1* positively contributes to longevity in a TOR-independent fashion in nematodes. As a readout of endoplasmic reticulum (ER) stress, we monitored the levels of P-eIF2α in WT and *efk-1* KO worms under normal feeding in the absence or presence of rapamycin or under caloric restriction. Caloric restriction greatly reduced the levels of P-eIF2α, whereas rapamycin also slightly decreased the levels of P-eIF2α in both WT and *efk-1* KO worms (Figure S7C). However, levels of P-eIF2α were similar in *efk-1* KO worms (Figure S7C), which corroborates our observations that eEF2K knockdown in A549 cells did not induce phosphorylation of eIF2α (Figure S5E). Therefore, the observed impairment of lifespan as the result of *efk-1* KO is unlikely to be caused by an increase in ER stress.

DISCUSSION

The faithful translation of mRNAs into proteins plays crucial roles in normal cell functions and organismal lifespan. During translation, amino acid misincorporation is estimated to happen at a rate between every 1 in 1,000 and 10,000 codons [5]. Over time, even low error rates in the synthesis of certain proteins, such as disease-associated ones, e.g., SOD1 (whose misfolding causes amyotrophic lateral sclerosis), can lead to accumulation of defective proteins even affecting the faithful transmission of genetic information [5]. In the 1960s–1970s, Orgel [35–37] proposed that increased rates of translation errors directly affect aging and lifespan. Although this theory was challenged in the 1970s–1980s [38–41], it was recently demonstrated that mRNA translation accuracy imposes strong evolutionary pressure [5, 6]. Indeed, mammals with low levels of translation inaccuracy live longer than those with high rates of translation errors [6].

Decades of studies have shown that caloric restriction can extend lifespan in invertebrates and in rodents. More recent studies have implicated key cellular components linked to the control of translation and that are regulated (directly or indirectly) by nutrients in modulating lifespan. These include mTORC1 [42] and its downstream substrates or effectors S6K1 ([43]; in mice), 4E-BP1 ([44]; in *D. melanogaster*), eIF4E ([45]; in *C. elegans*), and AMPK ([43]; in mice). Inhibition of mTOR signaling (a pathway that activates protein synthesis) extends lifespan in diverse organisms from yeast to mammals [7]. Furthermore, a range of conditions that slow down translation all extend lifespan in *C. elegans* [46].

Translation fidelity is assured by two main events: synthesis of the precisely paired aminoacyl-tRNAs by aminoacyl-tRNA synthetases, and the stringent selection of proper aminoacyl-tRNAs by the ribosomes during elongation. It has been shown that translation rates inversely correlate with cotranslation folding efficiency as well as translational accuracy [9]. Conn and Qian demonstrated that rates of mRNA mistranslation in TSC2 null cells (where mTORC1 signaling is constitutively activated [15]) are significantly higher than in WT cells [9]. They also showed that the impairment of translational fidelity in TSC2 null cells results from activation of the mTORC1-S6K1 pathway and that TSC2 null cells exhibit faster translation elongation [9]. However, prior to this, it was not known whether translation elongation directly impacted on translation fidelity or, if so, how this was linked to the mTORC1 pathway.

Here, we demonstrate faster translation due to the presence of surrounding codons with high usage rates (“fast codons”) leads to higher levels of mistranslation (Figures 1A–1C), whereas slower translation elongation reflecting low usage-rate codons (“slow codons”) correlates with reduced rates of translation errors. This provides further evidence that increased productivity

of the translation machinery occurs at the expense of poorer accuracy. Here we demonstrate that, under various stress conditions, where eEF2K is activated and slows down translation [27–29], eEF2K aids translational accuracy. Conversely, when mTORC1 signaling is active and switches off eEF2K to accelerate elongation, this reduces translation fidelity.

A reduction in eEF2K levels or its inactivation reduces the accuracy of decoding. mTORC1 can directly or indirectly drive the phosphorylation of several residues in eEF2K that impair its activity [14]; for example, S6K1 directly phosphorylates eEF2K at Ser366 and thereby inhibits its activity [47]. Importantly, we show that disabling eEF2K attenuates the ability of mTOR inhibitors to promote translational fidelity (Figures 2A–2E), thereby providing a molecular mechanism for the ability of mTORC1 to modulate the accuracy of protein synthesis [9]. Thus, surprisingly, although eEF2 does not itself mediate the step in elongation where aminoacyl-tRNAs are recruited to the A site, where a correct codon:anticodon match must be achieved, it does nevertheless link mTORC1 signaling and thus multiple stress conditions that activate eEF2K to the accuracy of elongation. These conditions include impaired glycolysis (Figures 1E and 1F), low pH (Figure 2C), nutrient deprivation (Figure 2D), and hypoxia (Figures 2E and 2F). Because levels of global protein synthesis were unaffected when eEF2K was knocked down (Figures S5G–S5J), translation fidelity appears to be affected mainly by the speed of elongation rather than the overall rate of protein production. Thus, our data point to eEF2K-mediated regulation of elongation helping to ensure accuracy rather than affecting overall rate of protein production, at least in the cells and under the conditions tested here.

AMPK is activated upon lack of metabolic energy and lies upstream of mTORC1 and eEF2K, suppressing or stimulating them, respectively [15, 48]. We show that the activation of AMPK also plays a positive regulatory role in translation fidelity; AMPK null MEFs exhibit impaired translation accuracy. This may reflect loss of the ability of AMPK to inhibit mTORC1 and stimulate eEF2K and/or the lower eEF2K protein levels in AMPK null cells [28, 29] (Figures 4A and 4B).

We also show that activation of eEF2K helps reduce initiation at codons similar to canonical AUG start sites, i.e., CUG or GUG (Figure 5). Initiation involves "scanning" by 40S ribosomal subunits and associated factors to seek appropriate start codons; this is facilitated by the fact that the relevant methionyl-initiator tRNA is already associated with them. Although the presence of secondary structure downstream of a start codon favors initiation from non-AUG codons and contributes to neurodegenerative diseases such as ALS (amyotrophic lateral sclerosis) and FXTAS (fragile X-associated tremor/ataxia syndrome) [49], our data actually suggest that impaired elongation, which would slow down ribosomes within the open reading frame, actually favors the "correct" choice of an AUG start codon, possibly because faster elongation (in cells where eEF2K has been knocked down) allows less time for selection of the optimal initiation codon (AUG) pair at the start site and acceptance of otherwise less favored ones such as GUG and CUG (Figure 5C).

A further key finding of this study is that *efk-1* is required for the lifespan extension that normally occurs in worms under nutritionally restricted conditions. Furthermore, because ablation of several aminoacyl (leucyl, arginyl, asparaginyl, or methionyl)-tRNA synthetases also decreases lifespan in nematodes, our data clearly demonstrate that factors implicated in regulating translational accuracy influence longevity (Figure 6). However, it should be noted that aminoacyl-tRNA synthetases and eEF2K (*efk-1* in nematodes) are proteins that are required for or regulate, respectively, mRNA translation. Although each has a specific function, they may exert pleiotropic effects, given the crucial importance of protein synthesis for cell physiology. Therefore, the decreased lifespan we observe in nematodes where *efk-1* or aminoacyl-tRNA synthetases were knocked down may be due to these effects. Also, although the correlation between slower elongation and greater lifespan holds true in nematodes and human cells, because TORC1 signaling is not known to regulate eEF2 in *C. elegans*, additional mechanisms must exist in them to account for the link between mTORC1 and longevity in nematodes.

Our data show that eEF2K promotes the fidelity of translation elongation and initiation, thereby providing a link between inhibition of mTORC1 signaling (which activates eEF2K in mammals) and the enhanced accuracy of protein synthesis. These data provide a mechanism for the very well-known association between impaired mTORC1 signaling or slower protein synthesis and greater lifespan.

STAR★METHODS

Detailed methods are provided in the online version of this paper and include the following:

- KEY RESOURCES TABLE
- CONTACT FOR REAGENT AND RESOURCE SHARING
- EXPERIMENTAL MODEL AND SUBJECT DETAILS
  - Generation of eEF2K KO MEFs
  - Cell culture
  - *C. elegans* husbandry
  - Fly husbandry
- METHOD DETAILS
  - Replication, randomization, blinding, sample-size and data/subject inclusion/exclusion
  - Cell treatment and lysis
  - SDS-PAGE and Western-blot analysis
  - Plasmids and transfection
  - Point mutagenesis
  - Polysome analysis
  - Luciferase assay
  - Real-time RT-PCR amplification analysis
  - *C. elegans* lifespan assays
  - Fly lifespan assays
  - Sequence design for characterization of the decoding system in mammalian cells
  - The Decoding Scheme
  - Modeling the human decoding system
  - Codon Decoding Speeds
  - Luciferase sequence design
  - Luciferase Sequences
  - Generation of CRISPR-directed eEF2K KO MDA-MB-231 cells
  - Global protein synthesis measurements

- *In vitro* refolding assay
- Proteasome activity measurement
- Primers

- QUANTIFICATION AND STATISTICAL ANALYSIS

SUPPLEMENTAL INFORMATION

Supplemental Information includes seven figures, one table, and one methods file and can be found with this article online at https://doi.org/10.1016/j.cub.2019.01.029.

ACKNOWLEDGMENTS

The authors would like to thank Dr. Daniel J. Peet (University of Adelaide, Adelaide, SA, Australia) for the use of the Edwards Instrument Hypoxia Workstation. We would like to thank the South Australian Health and Medical Research Institute (SAHMRI) for financial support. We would also like to acknowledge the CGC (Caenorhabditis Genetic Center; funded by the NIH Office of Research Infrastructure Programs, P40 OD010440) for their donation of nematode worms.

AUTHOR CONTRIBUTIONS

J.X. conducted most of the experiments. V.d.S.A. performed the *C. elegans* lifespan study. L.O. performed the *Drosophila* lifespan study. T.v.d.H., R.L., R.V.L., M.J.C., and X.W. also contributed data. All authors helped design the experiments. K.B.J., X.W., and C.G.P. provided supervision. All authors interpreted and analyzed the data. J.X., X.W., and C.G.P. wrote the manuscript.

DECLARATION OF INTERESTS

The authors declare no competing interests.

Received: May 21, 2018
Revised: December 12, 2018
Accepted: January 11, 2019
Published: February 14, 2019

REFERENCES

1. Kapur, M., and Ackerman, S.L. (2018). mRNA translation gone awry: translation fidelity and neurological disease. Trends Genet. *34*, 218–231.
2. Drummond, D.A., and Wilke, C.O. (2009). The evolutionary consequences of erroneous protein synthesis. Nat. Rev. Genet. *10*, 715–724.
3. Rodnina, M.V. (2012). Quality control of mRNA decoding on the bacterial ribosome. Adv. Protein Chem. Struct. Biol. *86*, 95–128.
4. Eyler, D.E., and Green, R. (2011). Distinct response of yeast ribosomes to a miscoding event during translation. RNA *17*, 925–932.
5. Drummond, D.A., and Wilke, C.O. (2008). Mistranslation-induced protein misfolding as a dominant constraint on coding-sequence evolution. Cell *134*, 341–352.
6. Ke, Z., Mallik, P., Johnson, A.B., Luna, F., Nevo, E., Zhang, Z.D., Gladyshev, V.N., Seluanov, A., and Gorbunova, V. (2017). Translation fidelity coevolves with longevity. Aging Cell *16*, 988–993.
7. Zoncu, R., Efeyan, A., and Sabatini, D.M. (2011). mTOR: from growth signal integration to cancer, diabetes and ageing. Nat. Rev. Mol. Cell Biol. *12*, 21–35.
8. Saxton, R.A., and Sabatini, D.M. (2017). mTOR signaling in growth, metabolism, and disease. Cell *169*, 361–371.
9. Conn, C.S., and Qian, S.B. (2013). Nutrient signaling in protein homeostasis: an increase in quantity at the expense of quality. Sci. Signal. *6*, ra24.
10. Sherman, M.Y., and Qian, S.B. (2013). Less is more: improving proteostasis by translation slow down. Trends Biochem. Sci. *38*, 585–591.
11. Redpath, N.T., Foulstone, E.J., and Proud, C.G. (1996). Regulation of translation elongation factor-2 by insulin via a rapamycin-sensitive signalling pathway. EMBO J. *15*, 2291–2297.
12. Ryazanov, A.G., Shestakova, E.A., and Natapov, P.G. (1988). Phosphorylation of elongation factor 2 by EF-2 kinase affects rate of translation. Nature *334*, 170–173.
13. Ryazanov, A.G., Pavur, K.S., and Dorovkov, M.V. (1999). Alpha-kinases: a new class of protein kinases with a novel catalytic domain. Curr. Biol. *9*, R43–R45.
14. Wang, X., Regufe da Mota, S., Liu, R., Moore, C.E., Xie, J., Lanucara, F., Agarwala, U., Pyr Dit Ruys, S., Vertommen, D., Rider, M.H., et al. (2014). Eukaryotic elongation factor 2 kinase activity is controlled by multiple inputs from oncogenic signaling. Mol. Cell. Biol. *34*, 4088–4103.
15. Inoki, K., Li, Y., Zhu, T., Wu, J., and Guan, K.L. (2002). TSC2 is phosphorylated and inhibited by Akt and suppresses mTOR signalling. Nat. Cell Biol. *4*, 648–657.
16. Wang, X., Xie, J., and Proud, C.G. (2017). Eukaryotic elongation factor 2 kinase (eEF2K) in cancer. Cancers (Basel) *9*, E162.
17. Richter, J.D., and Coller, J. (2015). Pausing on polyribosomes: make way for elongation in translational control. Cell *163*, 292–300.
18. Chu, D., Kazana, E., Bellanger, N., Singh, T., Tuite, M.F., and von der Haar, T. (2014). Translation elongation can control translation initiation on eukaryotic mRNAs. EMBO J. *33*, 21–34.
19. Mordret, E., Yehonadav, A., Barnabas, G.D., Cox, J., Dahan, O., Geiger, T., Lindner, A.B., and Pilpel, Y. (2018). Systematic detection of amino acid substitutions in proteome reveals a mechanistic basis of ribosome errors. bioRxiv. https://doi.org/10.1101/255943.
20. Jossé, L., Sampson, C.D.D., Tuite, M.F., Howland, K., and von der Haar, T. (2017). Codon-dependent translational accuracy controls protein quality in *Escherichia coli* but not in *Saccharomyces cerevisiae*. bioRxiv. https://doi.org/10.1101/200006.
21. von der Haar, T., Leadsham, J.E., Sauvadet, A., Tarrant, D., Adam, I.S., Saromi, K., Laun, P., Rinnerthaler, M., Breitenbach-Koller, H., Breitenbach, M., et al. (2017). The control of translational accuracy is a determinant of healthy ageing in yeast. Open Biol. *7*, 160291.
22. Branchini, B.R., Magyar, R.A., Murtiashaw, M.H., and Portier, N.C. (2001). The role of active site residue arginine 218 in firefly luciferase bioluminescence. Biochemistry *40*, 2410–2418.
23. Rakwalska, M., and Rospert, S. (2004). The ribosome-bound chaperones RAC and Ssb1/2p are required for accurate translation in *Saccharomyces cerevisiae*. Mol. Cell. Biol. *24*, 9186–9197.
24. Thompson, J.F., Hayes, L.S., and Lloyd, D.B. (1991). Modulation of firefly luciferase stability and impact on studies of gene regulation. Gene *103*, 171–177.
25. Dorovkov, M.V., Pavur, K.S., Petrov, A.N., and Ryazanov, A.G. (2002). Regulation of elongation factor-2 kinase by pH. Biochemistry *41*, 13444–13450.
26. Kruiswijk, F., Yuniati, L., Magliozzi, R., Low, T.Y., Lim, R., Bolder, R., Mohammed, S., Proud, C.G., Heck, A.J., Pagano, M., and Guardavaccaro, D. (2012). Coupled activation and degradation of eEF2K regulates protein synthesis in response to genotoxic stress. Sci. Signal. *5*, ra40.
27. Leprivier, G., Remke, M., Rotblat, B., Dubuc, A., Mateo, A.R., Kool, M., Agnihotri, S., El-Naggar, A., Yu, B., Somasekharan, S.P., et al. (2013). The eEF2 kinase confers resistance to nutrient deprivation by blocking translation elongation. Cell *153*, 1064–1079.
28. Xie, J., Mikolajek, H., Pigott, C.R., Hooper, K.J., Mellows, T., Moore, C.E., Mohammed, H., Werner, J.M., Thomas, G.J., and Proud, C.G. (2015). Molecular mechanism for the control of eukaryotic elongation factor 2 kinase by pH: role in cancer cell survival. Mol. Cell. Biol. *35*, 1805–1824.
29. Moore, C.E., Mikolajek, H., Regufe da Mota, S., Wang, X., Kenney, J.W., Werner, J.M., and Proud, C.G. (2015). Elongation factor 2 kinase is regulated by proline hydroxylation and protects cells during hypoxia. Mol. Cell. Biol. *35*, 1788–1804.

30. Chresta, C.M., Davies, B.R., Hickson, I., Harding, T., Cosulich, S., Critchlow, S.E., Vincent, J.P., Ellston, R., Jones, D., Sini, P., et al. (2010). AZD8055 is a potent, selective, and orally bioavailable ATP-competitive mammalian target of rapamycin kinase inhibitor with in vitro and in vivo antitumor activity. Cancer Res. *70*, 288–298.

31. Kramer, E.B., and Farabaugh, P.J. (2007). The frequency of translational misreading errors in *E. coli* is largely determined by tRNA competition. RNA *13*, 87–96.

32. Stewart, J.D., Cowan, J.L., Perry, L.S., Coldwell, M.J., and Proud, C.G. (2015). ABC50 mutants modify translation start codon selection. Biochem. J. *467*, 217–229.

33. Alves, V. (2015). Reactivity of vertebrate-directed phospho-eEF2 antibody against the *Caenorhabditis elegans* orthologue phospho-EEF-2. F1000Res. *4*, 902.

34. Vellai, T., Takacs-Vellai, K., Zhang, Y., Kovacs, A.L., Orosz, L., and Müller, F. (2003). Genetics: influence of TOR kinase on lifespan in *C. elegans*. Nature *426*, 620.

35. Orgel, L.E. (1973). Ageing of clones of mammalian cells. Nature *243*, 441–445.

36. Orgel, L.E. (1970). The maintenance of the accuracy of protein synthesis and its relevance to ageing: a correction. Proc. Natl. Acad. Sci. USA *67*, 1476.

37. Orgel, L.E. (1963). The maintenance of the accuracy of protein synthesis and its relevance to ageing. Proc. Natl. Acad. Sci. USA *49*, 517–521.

38. Edelmann, P., and Gallant, J. (1977). On the translational error theory of aging. Proc. Natl. Acad. Sci. USA *74*, 3396–3398.

39. Wojtyk, R.I., and Goldstein, S. (1980). Fidelity of protein synthesis does not decline during aging of cultured human fibroblasts. J. Cell. Physiol. *103*, 299–303.

40. Mori, N., Hiruta, K., Funatsu, Y., and Goto, S. (1983). Codon recognition fidelity of ribosomes at the first and second positions does not decrease during aging. Mech. Ageing Dev. *22*, 1–10.

41. Szajnert, M.F., and Schapira, F. (1983). Properties of purified tyrosine aminotransferase from adult and senescent rat liver. Gerontology *29*, 311–319.

42. Harrison, D.E., Strong, R., Sharp, Z.D., Nelson, J.F., Astle, C.M., Flurkey, K., Nadon, N.L., Wilkinson, J.E., Frenkel, K., Carter, C.S., et al. (2009). Rapamycin fed late in life extends lifespan in genetically heterogeneous mice. Nature *460*, 392–395.

43. Selman, C., Tullet, J.M., Wieser, D., Irvine, E., Lingard, S.J., Choudhury, A.I., Claret, M., Al-Qassab, H., Carmignac, D., Ramadani, F., et al. (2009). Ribosomal protein S6 kinase 1 signaling regulates mammalian life span. Science *326*, 140–144.

44. Zid, B.M., Rogers, A.N., Katewa, S.D., Vargas, M.A., Kolipinski, M.C., Lu, T.A., Benzer, S., and Kapahi, P. (2009). 4E-BP extends lifespan upon dietary restriction by enhancing mitochondrial activity in *Drosophila*. Cell *139*, 149–160.

45. Syntichaki, P., Troulinaki, K., and Tavernarakis, N. (2007). eIF4E function in somatic cells modulates ageing in *Caenorhabditis elegans*. Nature *445*, 922–926.

46. Hansen, M., Taubert, S., Crawford, D., Libina, N., Lee, S.J., and Kenyon, C. (2007). Lifespan extension by conditions that inhibit translation in *Caenorhabditis elegans*. Aging Cell *6*, 95–110.

47. Wang, X., Li, W., Williams, M., Terada, N., Alessi, D.R., and Proud, C.G. (2001). Regulation of elongation factor 2 kinase by p90(RSK1) and p70 S6 kinase. EMBO J. *20*, 4370–4379.

48. Horman, S., Browne, G., Krause, U., Patel, J., Vertommen, D., Bertrand, L., Lavoinne, A., Hue, L., Proud, C., and Rider, M. (2002). Activation of AMP-activated protein kinase leads to the phosphorylation of elongation factor 2 and an inhibition of protein synthesis. Curr. Biol. *12*, 1419–1423.

49. Kearse, M.G., Green, K.M., Krans, A., Rodriguez, C.M., Linsalata, A.E., Goldstrohm, A.C., and Todd, P.K. (2016). CGG repeat-associated non-AUG translation utilizes a cap-dependent scanning mechanism of initiation to produce toxic proteins. Mol. Cell *62*, 314–322.

50. Xie, J., Shen, K., Lenchine, R.V., Gethings, L.A., Trim, P.J., Snel, M.F., Zhou, Y., Kenney, J.W., Kamei, M., Kochetkova, M., et al. (2018). Eukaryotic elongation factor 2 kinase upregulates the expression of proteins implicated in cell migration and cancer cell metastasis. Int. J. Cancer *142*, 1865–1877.

51. Anderson, L.L., Mao, X., Scott, B.A., and Crowder, C.M. (2009). Survival from hypoxia in *C. elegans* by inactivation of aminoacyl-tRNA synthetases. Science *323*, 630–633.

52. Dietzl, G., Chen, D., Schnorrer, F., Su, K.C., Barinova, Y., Fellner, M., Gasser, B., Kinsey, K., Oppel, S., Scheiblauer, S., et al. (2007). A genome-wide transgenic RNAi library for conditional gene inactivation in *Drosophila*. Nature *448*, 151–156.

53. Porta-de-la-Riva, M., Fontrodona, L., Villanueva, A., and Cerón, J. (2012). Basic *Caenorhabditis elegans* methods: synchronization and observation. J. Vis. Exp. (64), e4019.

54. Chan, P.P., and Lowe, T.M. (2009). GtRNAdb: a database of transfer RNA genes detected in genomic sequence. Nucleic Acids Res. *37*, D93–D97.

55. Grosjean, H., de Crécy-Lagard, V., and Marck, C. (2010). Deciphering synonymous codons in the three domains of life: co-evolution with specific tRNA modification enzymes. FEBS Lett. *584*, 252–264.

56. Czerwoniec, A., Dunin-Horkawicz, S., Purta, E., Kaminska, K.H., Kasprzak, J.M., Bujnicki, J.M., Grosjean, H., and Rother, K. (2009). MODOMICS: a database of RNA modification pathways. 2008 update. Nucleic Acids Res. *37*, D118–D121.

57. Plant, E.P., Nguyen, P., Russ, J.R., Pittman, Y.R., Nguyen, T., Quesinberry, J.T., Kinzy, T.G., and Dinman, J.D. (2007). Differentiating between near- and non-cognate codons in *Saccharomyces cerevisiae*. PLoS ONE *2*, e517.

58. Pavon-Eternod, M., Gomes, S., Geslain, R., Dai, Q., Rosner, M.R., and Pan, T. (2009). tRNA over-expression in breast cancer and functional consequences. Nucleic Acids Res. *37*, 7268–7280.

59. Chu, D., Barnes, D.J., and von der Haar, T. (2011). The role of tRNA and ribosome competition in coupling the expression of different mRNAs in *Saccharomyces cerevisiae*. Nucleic Acids Res. *39*, 6705–6714.

60. Kothe, U., and Rodnina, M.V. (2007). Codon reading by tRNAAla with modified uridine in the wobble position. Mol. Cell *25*, 167–174.

61. Keller, G.A., Gould, S., Deluca, M., and Subramani, S. (1987). Firefly luciferase is targeted to peroxisomes in mammalian cells. Proc. Natl. Acad. Sci. USA *84*, 3264–3268.

STAR★METHODS

KEY RESOURCES TABLE

REAGENT or RESOURCE	SOURCE	IDENTIFIER
Antibodies		
P-eEF2 Thr56	Eurogentec	Customized
eEF2	Cell Signaling Technology	2332S; RRID:AB_10693546
eEF2K	Eurogentec	Customized
P-rpS6 Ser240/Ser244	Cell Signaling Technology	2215S; RRID:AB_331682
rpS6	Santa Cruz Biotechnology	SC74459; RRID:AB_1129205
P-S6K1 Thr389	Cell Signaling Technology	9205S; RRID:AB_330944
S6K1	Santa Cruz Biotechnology	SC230; RRID:AB_632156
4EBP1	Cell Signaling Technology	9452S; RRID:AB_331692
P-PKB Ser473	Cell Signaling Technology	9271S; RRID:AB_329825
PKB	Cell Signaling Technology	9272S; RRID:AB_329827
P-Erk1/2 Thr202/Tyr204	Cell Signaling Technology	9101S; RRID:AB_331646
ERK1/2	Cell Signaling Technology	9102S; RRID:AB_330744
P-ACC Ser79	Cell Signaling Technology	3661S; RRID:AB_330337
ACC	Cell Signaling Technology	4190S; RRID:AB_10547752
P-AMPKα Ser172	Cell Signaling Technology	2535S; RRID:AB_331250
AMPK	Cell Signaling Technology	2532S; RRID:AB_330331
Ubiquitin	Cell Signaling Technology	3936S; RRID:AB_331292
SARS	SA	AV40654-100UL; RRID:AB_1856583
P-eIF2α Ser51	Cell Signaling Technology	9721S; RRID:AB_329825
eIF2α	Cell Signaling Technology	5324S; RRID:AB_10692650
Firefly luciferase	Sigma-Aldrich	L0159; RRID:AB_260379
β-Actin	Sigma-Aldrich	A5441; RRID:AB_476744
α-tubulin	Sigma-Aldrich	T6074; RRID:AB_477582
Chemicals, Peptides, and Recombinant Proteins		
2-DG	Sigma-Aldrich	D8375-1G
Rapamycin	Sigma-Aldrich	R0395
AZD8055	Selleckchem	S1555
Trans ^{35}S-Label	MP Biomedicals	015100607
QuantiLum Recombinant Luciferase	Promega	E1701
pfu polymerase	Promega	M7741
Critical Commercial Assays		
Dual-Glo Luciferase Assay System	Promega	E2920
Proteasome-Glo chymotrypsin-like cell based assay system	Promega	G8660
Super-Script III First-Strand synthesis system	Life Technologies	18080051
PrecisionPLUS qPCR SYBR green dye mix	PrimerDesign	PPLUS-machine type-20ML
Dynabeads CD4 Positive Isolation Kit	Thermofisher Scientific	11331D
Experimental Models: Cell Lines		
A549	Janssen Pharmaceutica	[28]; RRID:CVCL_0023
HCT116	Janssen Pharmaceutica	[28]; RRID:CVCL_0291
MDA-MB-231	[50]	[50]; RRID:CVCL_0062
HEK293	[28]	[28]; RRID:CVCL_0045

(*Continued on next page*)

Continued

REAGENT or RESOURCE	SOURCE	IDENTIFIER
Experimental Models: Organisms/Strains		
eEF2K$^{+/+}$ and *eEF2K*$^{-/-}$ *Mus musculus* (C57BL/6J; female)	[29]	[29]
Caenorhabditis elegans [N2 Bristol (wild isolate), efk-1 (0k3609)]	Caenorhabditis Genetic Center	[33]
Caenorhabditis elegans (*lrs-1, mrs-2, kars-1, rrs-1 and nrs-1)*	C. Michael Crowder, Washington University School of Medicine, MO, USA	[51]
Drosophila melanogaster (w1118, Actin-Gal4/CyO; tub-GAL80ts; male)	Bloomington Drosophila Stock Center	4414; 7017
Drosophila melanogaster (LeuRS GD knockdown; male)	Vienna Drosophila Research Centre	v34498
Oligonucleotides		
Please see Table S1		N/A
Software and Algorithms		
GraphPad Prism 8	GraphPad	https://www.graphpad.com/scientific-software/prism/; RRID:SCR_002798
Image Studio Lite 4.0	Li-Cor	https://www.licor.com/bio/products/software/image_studio_lite/; RRID:SCR_013715
WinDaq Waveform Browser	DATAQ instruments	https://www.dataq.com/products/windaq/
Other		
GloMax Discover Multimode Microplate Reader	Promega	GM3000
Victor3 1420 multilabel counter	Perkin Elmer	Victor3 1420
Li-Cor Odyssey imaging system	Li-Cor	https://www.licor.com/bio/products/imaging_systems/odyssey
Hypoxia workstation	Edward Instruments	N/A
UA-6 UV/VIS detector	ISCO	UA-6
CFX Connect Real-Time system	Bio-Rad	1855201
BD FACSAria Fusion flow cytometer	Becton, Dickinson & Company	BD FACSARIA FUSION
GeneArt CD4 CRISPR Nuclease Vector	Thermofisher Scientific	A21175

CONTACT FOR REAGENT AND RESOURCE SHARING

Further information and requests for resources and reagents should be directed to and will be fulfilled by the Lead Contact, Christopher G. Proud (Christopher.Proud@sahmri.com).

EXPERIMENTAL MODEL AND SUBJECT DETAILS

Generation of eEF2K KO MEFs

C57BL/6J Mice were group-housed with littermates at 24°C and under 12 h light/12 h dark cycle, fed with standard food and water provided *ad libitum* (Biomedical Research Facility, University of Southampton), in line with the United Kingdom Animals (Scientific Procedures) Act 1986. Mouse embryonic fibroblasts (MEFs, fetus) from eEF2K KO female mice [29] and their WT counterparts were prepared from embryos at embryonic day 13.5.

Cell culture

A549 (male) and HCT116 (male) cells expressing inducible short hairpin RNA (shRNA) against eEF2K were generously provided by Janssen Pharmaceutica (Beerse, Belgium) [28]. Authenticity of A549, HCT116, MDA-MB-231 (female) [50] and HEK293 (fetus) cells [28] (STR profile analysis) was performed by Garvan Institute (Sydney, Australia) on the 15th/Aug/2015. Cells were maintained in high glucose (4.5 g/L) Dulbecco's modified Eagle medium (DMEM) containing 10% (vol/vol) fetal bovine serum (FBS) and 1% penicillin-streptomycin.

C. elegans husbandry

C. elegans strain N2 Bristol (wild isolate), *efk-1* (*0k3609*) (CGC, #RB2588 [33]) obtained from CGC (Caenorhabditis Genetic Center, University of Minnesota, Minneapolis, USA), were maintained at 15°C on nematode growth media (NGM) and propagated and manipulated on *E. coli* stain OP50.

RNAi bacterial strains (*lrs-1*, *mrs-2*, *kars-1*, *rrs-1* and *nrs-1*) were kindly provided by Crowder Lab [51] and were grown overnight in LB broth with 50 μg/mL ampicillin and 10 μg/mL tetracycline at 37°C and then diluted 1:100 in LB with the same antibiotics. Strains were then grown at 37°C until reaching an OD of 0.4. A total of 100 μL of the RNAi bacteria plus 0.4 mM IPTG and ampicilin/tetracycline was added to each NGM plate. After 18 h of bacterial growth at 23°, L1 nematodes were grown to young adulthood (L4 worms), unless otherwise noted, on the RNAi plates then assayed.

Fly husbandry

Stocks used in this study were obtained from the Bloomington *Drosophila* Stock Center (NIH P40OD018537): w^{1118}, Actin-Gal4/CyO (#4414), tub-GAL80^{ts} (*#7017)* or Vienna *Drosophila* Research Centre (https://stockcenter.vdrc.at/control/main): LeuRS GD knockdown (v34498) [52] *D. melanogaster* stocks were maintained on fortified (F1) medium composed of 1% agar, 1% glucose, 6% fresh yeast, 9.3% molasses, 8.4% coarse semolina, 0.9% acid mix and 1.7% tegosept. Stocks were kept at 18°C, crosses were carried out at 18°C and male adult flies were aged at 29°C for lifespan assays.

All animals used in this study were healthy and immunocompetent, they were not involved in previous procedures and did not present any signs of drug or test naivety.

METHOD DETAILS

Replication, randomization, blinding, sample-size and data/subject inclusion/exclusion

Data were not analyzed blindly. At least two independent replicates were performed for each experiment (please see figure legends for the exact number). No specific method was used to predetermine the number of samples. We did not exclude any data/subject.

Cell treatment and lysis

To induce the knockdown of eEF2K, A549 or HCT116 cells were cultured with 1 M isopropyl-β-D-1thiogalactopyranoside (IPTG) for 5 days prior to use. For 2-deoxyglucose (2-DG) treatment, cells were pre-cultured in low glucose (1 g/L) DMEM for 1 h before the addition of 10 mM 2-DG for the indicated periods of times. For pH-buffered medium, pH was adjusted by adding different concentrations of $NaHCO_3$. For culturing cells in Dulbecco's Phosphate Buffered Saline (DPBS) or rapamycin/AZD8055 treatment, medium was changed just before the experiment. Hypoxia experiments were performed using a humidified hypoxia workstation (Edward Instruments, Sydney, NSW, Australia). After treatment, cells were lysed in ice-cold lysis buffer containing 1% (v/v) Triton X-100, 20 mM Tris-HCl (pH 7.5), 150 mM NaCl, 1 mM EDTA, 1 mM EGTA, 2.5 mM $NaH_2P_2O_7$, 1 mM β-glycerophosphate, 1 mM Na_3VO_4 and protease inhibitor cocktail (1X, Sigma-Aldrich, Castle Hill, NSW, Australia). Lysates were spun at 16,000 x *g* for 10 min, the supernatants were kept and total protein concentration was quantified by the Bradford assay (Bio-Rad Laboratories, Gladesville, NSW, Australia).

SDS-PAGE and Western-blot analysis

Laemmli sample buffer was added to cell lysates and the mixture was boiled at 100°C for 4 min before loading on to the SDS-PAGE gel (Protean 3 mini-slab gel system, Bio-Rad Laboratories). Proteins were then transferred to nitrocellulose membranes. Membranes were blocked in phosphate-buffered saline (PBS) containing 0.1% Tween-20 (PBST) and 5% skimmed milk for 1 h, washed thrice in PBST, followed by incubation with primary antibody overnight at 4°C. Membranes were then washed twice in PBST and incubated with fluorescently tagged secondary antibody for 1 h, washed again thrice in PBST and fluorescent signals were visualized using Li-Cor Odyssey imaging system (Millennium Science, Surrey Hills, VIC, Australia). See Key Resources Table for a list of primary antibodies used in this study.

Plasmids and transfection

Cells were transfected with luciferase DNA constructs [32] (Methods S1; Figures S1A–S1E) using Lipofectamine 3000 (Life Technologies, Adelaide, SA, Australia).

Point mutagenesis

Point mutations were introduced by PCR mutagenesis using pfu polymerase (Promega, Sydney, NSW, Australia). Please see Table S1 for a full list of mutagenesis primers.

Polysome analysis

Cells were lysed in polysome lysis buffer [10 mM NaCl, 10 mM $MgCl_2$, 10 mM Tris-HCl, pH 7.5, 1% (v/v) Triton X-100, 1% sodium deoxycholate, 36 U/mL RNase inhibitor, 1 mM dithiothreitol] and layered in a 20%–50% (w/v) sucrose gradient in 30 mM Tris-HCl, pH 7.5, 100 mM NaCl and 10 mM $MgCl_2$, followed by centrifugation at 234 000 x *g* for 150 min. The absorbance at 254 nm across the sucrose gradient was continuously monitored using a UA-6 UV/VIS detector (Isco). Data was analyzed using the WinDaq Waveform Browser software (DataQ instruments).

Luciferase assay

Fluc activity was measured with luciferase reporter assay systems (Promega) on a GloMax-discover multimode detection system (Promega) following the manufacturer's instructions.

Real-time RT-PCR amplification analysis

Total RNA was extracted using TRIzol (Life Technologies). cDNA was synthesized using Super-Script III First-Strand (synthesis system for RT-PCR) from Life Technologies with oligo(dT)$_{20}$. Samples were analyzed in triplicate (for each experiment) with SYBR green dye mix (PrimerDesign, Camberley, Hampshire, UK) on a CFX Connect Real-Time system (Bio-Rad Laboratories). The comparative threshold cycle (C_T) method was used to determine the amount of specific mRNAs compared with level of *B2M* (human or mouse cells) or *RP49* (*Drosophila*) RNA as the house-keeping genes, respectively.

C. elegans lifespan assays

Worms were tightly synchronized on OP50 seeded NGM plates [53] and eggs were incubated at 15°C until they reached the L1 stage. L4 worms were transferred to NGM seeded with OP50 and incubated at 23°C until reached L4 stage. 80 worms of each strain were picked to several NGM plates (20 worms/plate), supplemented with rapamycin and 5′-fluorodeoxyuridine (FUdR), and maintained at 25°C. Animals were transferred to fresh OP50 [live or heat-killed (HK)] plates every 1-2 days. Worms that crawled off the plate, bagged, or ruptured were censored. For all experiments, ampicillin (100 μg/mL) was added to the medium to selectively prevent growth of *E. coli* OP50 carried over on transfer of worms. Kaplan Meier survival curves were generated and statistically compared using GraphPad Prism Software (GraphPad Software, San Diego, CA, USA).

Fly lifespan assays

Adult flies were generated by crossing virgin females that were either w^{1118} (control) or UAS-*LeuRS GD* (LeuRS knockdown) to *Actin-GAL4/CyO;tub-GAL80^{ts}/TM6B* males. Crosses were carried out at 18°C with care taken not to overcrowd vials. Male adult flies were collected into vials (25 flies per vial) and shifted to 29°C for aging then turned onto new food every 2-3 days with the number of deaths recorded at every turn. Survival curve comparisons were graphed and analyzed using GraphPad Prism with significance of difference survival curves determined using Log Rank (Mantel-Cox) test.

Sequence design for characterization of the decoding system in mammalian cells

tRNA identities are from the genomic tRNA database [54], based on a tRNAscan-SE. Analysis of the *Homo sapiens* genome (hg18 - NCBI Build 36.1 Mar 2006). Anticodon modifications were introduced as reviewed in [55] and symbols for modified nucleotides are as used in the Modomics database [56].

The Decoding Scheme

All possible relationships between codons and tRNAs were examined and assigned to one of four possible categories: WC-cognate if all nucleotides of the anticodon can form Watson:Crick (WC) base pairs with the codon; wobble-cognate if the last two nucleotides of the anticodon can form WC base pairs and the first can form a wobble base pair; near-cognate if the middle nucleotide of the anticodon can form a WC base pair with the codon and the first and third nucleotides can form wobble base pairs (following rules established in [57]); or non-cognate for all other tRNAs. The results are summarized in Figure S1F.

Modeling the human decoding system

From the scheme in Figure S1F, from individual tRNA expression levels in HEK293 cells as determined by microarray in [58], and from a total tRNA concentration of 190 μM (based on the value for baker's yeast [59]), concentrations of the four classes of tRNAs were determined for each codon. The resulting concentrations were used as parameters for simulations of the decoding process for each codon. The rate parameters for WC-cognate, near-cognate and non-cognate tRNAs were as in our previous models.

For the wobble-cognate class, a new set of parameters was used based on the biochemical measurements reported in [60]. This extends the previously used model to include a more realistic behavior of wobble-decoding tRNAs (especially their significant rejection rate, which delays the decoding process beyond the near-cognate:cognate ratio).

Codon Decoding Speeds

The average of 1,000 individual stochastic simulation results were used to determine the average decoding time for each codon, as predicted by our model. The resulting average decoding times are shown in Figure S1G.

Luciferase sequence design

Based on the data in Figure S1G, sequences were designed encoding Firefly Luciferase protein, using only the fastest (hsa_maxCFLuc) or slowest (hsa_minCFLuc) possible codons. In all constructs, the luciferase protein is an engineered version lacking the C-terminal three amino acids of the WT protein [18], which removes the peroxisomal localization signal [61] leading to cytoplasmic expression.

Figure S1H compares the speed of the dis-optimized (left) and optimized (right) sequences with the original firefly luciferase (staCFLuc, middle). In this figure, the decoding speed of individual codons is plotted against the codon position. Speed of individual codons is plotted as gray circles, black lines display the smoothed local decoding speed.

Luciferase Sequences

Please see Methods S1 for details.

Generation of CRISPR-directed eEF2K KO MDA-MB-231 cells

The eEF2K KO CRISPR targeting vector was the GeneArt CD4 CRISPR Nuclease Vector (ThermoFisher Scientific, Scoresby, VIC, Australia). Guide ssDNA sequence was 5′-AGTGAGCGGTATAGCTCCAG-3′. Cells were transfected with the CRISPR vector by nucleofection (Lonza, Mt Waverley, Australia). After 72 h, CD4-positive cells were enriched using magnetic CD4 Dynabeads (ThermoFisher Scientific) and then sorted into individual wells of 96-well plates using a BD FACSFusion flow cytometer (Becton, Dickinson & Company, Wayville, SA, Australia). Positive clones were selected by immunoblotting analysis for the absence of P-eEF2, and were further confirmed by Sanger sequencing analysis (performed by the Australian Genome Research Facility, Adelaide, Australia).

Global protein synthesis measurements

Cells were preincubated in either DPBS or DMEM lacking glucose, $NaHCO_3$, methionine, and cysteine free (customized by Labtech International, Heathfield, UK), supplemented with 10% (v/v) FBS, 1% penicillin-streptomycin, 1 (for 2-DG treatment) or 4.5 (all other treatments) g/L glucose, and 44 mM $NaHCO_3$ (except for pH treatments) for 1 h. For pH treatments, pH was adjusted by adding different concentrations of $NaHCO_3$. Where indicated, 10 mM 2-DG or 1 μM AZD8055 was added to the cells. 10 μCi [^{35}S]methionine-cysteine (Trans ^{35}S-Label, MP Biomedicals, Seven Hills, NSW, Australia) were also added and cells were further incubated for either 1 (for DPBS treatment) or 16 (for all other treatments) h. Incorporated radioactivity was then determined by scintillation counting.

In vitro refolding assay

QuantiLum Recombinant Luciferase (Promega, Sydney, Australia) was diluted in lysis buffer at 50 μg/mL and then denatured at 42°C and 1000 rpm for 15 min. Denatured Fluc was added to cell lysates for a final concentration of 16.5 μg/mL. Refolding was conducted at room temperature and 1000 rpm for the indicated periods of time. Fluc activity was monitored with luciferase reporter assay system (Promega) on a Victor3 1420 multilabel counter (Perkin Elmer) following the manufacturer's instructions. Fluc activity in lysis buffer alone was also measured to exclude spontaneous refolding of denatured Fluc.

Proteasome activity measurement

Intracellular chymotrypsin activity was monitored using Proteasome-Glo chymotrypsin-like cell based assay system (Promega) on a Victor3 1420 multilabel counter (Perkin Elmer) following manufacturer's instructions.

Primers

Please see Table S1 for details.

QUANTIFICATION AND STATISTICAL ANALYSIS

All bar graphs and line plots show means and standard errors. Statistical analysis were performed using a one-way or two-way ANOVA analysis of variance with an unpaired Student's t test with the means of independent experiments unless otherwise specified. GraphPad Prism software package was used to calculate p values. To indicated the data met assumptions of the statistical approach: *: $0.01 \leq p < 0.05$; **: $0.001 \leq p < 0.01$; ***: $p < 0.001$. For simplicity, not all statistical significances were shown.